Potential ultrahigh pressure polymorphs of ABX_3-type compounds

Koichiro Umemoto and Renata M. Wentzcovitch
Minnesota Supercomputing Institute and Department of Chemical Engineering and Materials Science, University of Minnesota, 421 Washington Avenue SE, Minneapolis, Minnesota 55455, USA

(Received 25 August 2006; revised manuscript received 11 October 2006; published 11 December 2006)

We have identified by first-principles computations two dynamically stable structures that are candidate ultrahigh pressure polymorphs of ABX_3-type compounds. To our knowledge, they have not been experimentally observed yet. They are produced by *metastable* pressure-induced transformations in *Cmcm* $NaMgF_3$, a postperovskite phase. The first transition to a *Pmcn* structure is related to a soft phonon mode in postperovskite. The second one is a regular enthalpically driven transition from *Pmcn* to a $P6_3/mmc$ structure. In $NaMgF_3$ these phases are metastable with respect to the dissociation into CsCl-type NaF and cotunnite-type MgF_2. However, other ABX_3-type compounds may favor these phases over the dissociation products. Even in $NaMgF_3$, the *Pmcn* phase might be observed at low temperatures.

DOI: 10.1103/PhysRevB.74.224105 PACS number(s): 91.60.Gf, 83.80.Nb, 64.70.Kb, 63.20.Dj

I. INTRODUCTION

The surprising discovery of a pressure-induced transition in $MgSiO_3$ perovskite (PV with *Pbnm* symmetry) to $CaIrO_3$-type postperovskite (PPV with *Cmcm* symmetry) at pressure-temperature (PT) conditions similar to those expected near the core-mantle boundary of the Earth (at ~125 GPa and 2500 K)[1–3] has increased scientific interest in the $CaIrO_3$-type structure itself. The PPV transition raises a new question: what would be the next phase transition from the $CaIrO_3$-type structure? Since ABX_3 PPV consists of BX_3 layers intercalated with A atoms, it is natural to expect still another phase transition to a more close-packed structure. However, no *post*-PPV structure has been identified experimentally so far. In contrast, first-principles computations have predicted the pressure-induced dissociation of $MgSiO_3$ PPV into CsCl-type MgO and cotunnite-type SiO_2 at ~1.1 TPa, a pressure relevant for the giant planets.[4] The same type of dissociation has also been predicted at ~40 GPa in $NaMgF_3$ PPV, a low-pressure analog of $MgSiO_3$.[5] These predictions, however, do not guarantee that *all* ABX_3 PPVs should dissociate. Some of them might prefer to undergo a post-PPV transition to another ABX_3 polymorph before dissociating. A post-PPV phase might also be observed metastably at low temperatures if the energy barrier for dissociation is large, or if the dissociation products (AX and BX_2) have a limited stability range.

In this paper, we propose two potential candidate structures for a post-PPV phase. They have symmetries *Pmcn* and $P6_3/mmc$ and larger cation coordination numbers than the *Cmcm* PPV structure. To our knowledge, these structures have not been identified experimentally in any material. They are dynamically stable phases of $NaMgF_3$, but metastable with respect to the dissociation products. Our predictions of the dissociation and transformations to these phases might help experimentalists identify these structures in ABX_3-type compounds under high pressure in the future.

We use the same computational methods[6–11] and pseudopotentials[12] cited and reported in Ref. 5. The numbers of formula units in the unit cells, **k** points in the irreducible wedge, and **q** points at which dynamical matrices are computed are (2, 6, 6) for *Cmcm*, (4, 2, 8) for *Pmcn*, and (2, 6, 4) for $P6_3/mmc$ $NaMgF_3$.

II. RESULTS AND DISCUSSION

Figure 1 shows the pressure dependence of lattice constants of *Cmcm* $NaMgF_3$ [Fig. 2(a)] under static compression. Up to ~80 GPa, all lattice constants decrease as well as their compressibilities. At ~80 GPa, a and c start increasing *under compression*, implying there is a change in compression mechanism. This change is captured also in the pressure dependence of the phonon dispersion (Fig. 3). The lowest acoustic phonon branch softens with increasing pressure and eventually becomes unstable around the Y point of the Brillouin zone beyond ~100 GPa, while all other phonon frequencies increase with pressure. This zone-edge soft mode

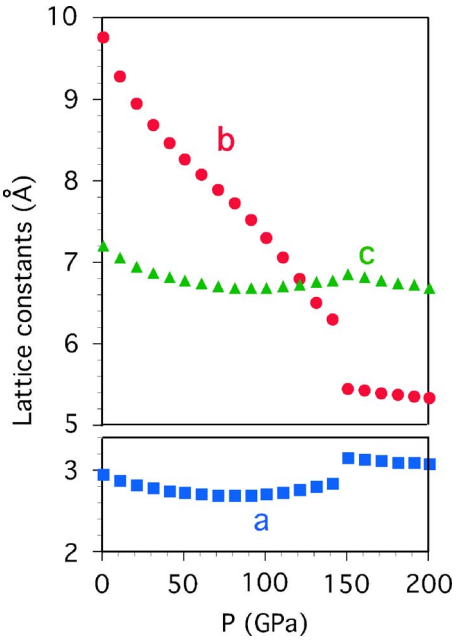

FIG. 1. (Color online) Pressure dependence of lattice constants of *Cmcm* $NaMgF_3$. Pressures are static values.

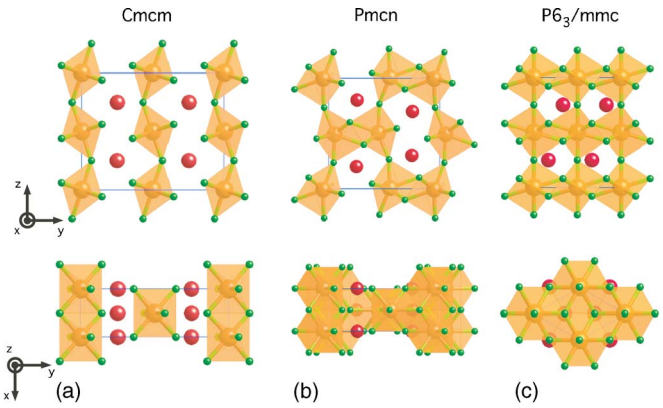

FIG. 2. (Color online) Crystal structure of $NaMgF_3$ with the symmetry (a) *Cmcm*, (b) *Pmcn*, and (c) $P6_3/mmc$. Red, orange, and green spheres denote Na, Mg, and F atoms, respectively. For simplicity, only Mg–F bonds are drawn here.

induces atomic displacements in a doubled unit cell (Fig. 4). Structural optimization after applying these soft mode displacements leads to a new crystal structure [Fig. 2(b)]. The new phase has a simple orthorhombic unit cell with 20 atoms and *Pmcn* symmetry, a subgroup of the *Cmcm* space group. It is clear from the charge density shown in Fig. 5 that new bonds appear between Mg and F in adjacent layers. In this transition, the Mg coordination number increases from 6 to 7 and the structural unit becomes MgF_7. The charge densities between Na and F also increase. Hence the bonding between layers strengthens, the bulk modulus increases from 282 GPa in the *Cmcm* phase to 292 GPa in the *Pmcn* phase at 50 GPa, and the acoustic phonon frequencies increase (Figs. 3 and 6). In contrast, the increase in Mg coordination number weakens individual Mg–F bonds. This gives rise to longer Mg–F bond lengths than those of *Cmcm* $NaMgF_3$ and to a decrease of the high optical phonon frequencies (Figs. 3 and 6). The shortest and average Mg–F bond lengths are 1.787 and 1.828 Å in the *Cmcm* phase and 1.877 and 1.904 Å in the *Pmcn* phase, respectively. It is this increase in Mg–F bond lengths through the transition that increases the lattice constants a and c. The new bonds between layers decrease the lattice constant b (Table I). Figure 7(a) shows that the static transition pressure from *Cmcm* to *Pmcn* $NaMgF_3$ is 43.3 GPa. *Pmcn* $NaMgF_3$ is dynamically stable, since all phonon frequencies are real (Fig. 3). When the *Pmcn* phase is decompressed, Mg–F bonds between layers break down and it transforms back to the *Cmcm* phase at 20 GPa. *Pmcn* $NaMgF_3$ is clearly metastable below 43.3 GPa because there are no soft modes.

Under *static compression*, which cannot induce any symmetry reduction in this type of calculation, *Cmcm* $NaMgF_3$ does not transform to the *Pmcn* structure. Instead, it continues to have *Cmcm* symmetry but in a configuration of unstable equilibrium with respect to the Y soft mode displacement. The lattice constants a and c continue to increase, while b continues to decrease. Then, at ~150 GPa, there are abrupt jumps of all lattice constants (Fig. 1). b becomes equal to $\sqrt{3}a$ which means the structure has acquired hexagonal symmetry. The resulting structure is shown in Fig. 2(c). The symmetry is $P6_3/mmc$, which is a supergroup of *Cmcm*.

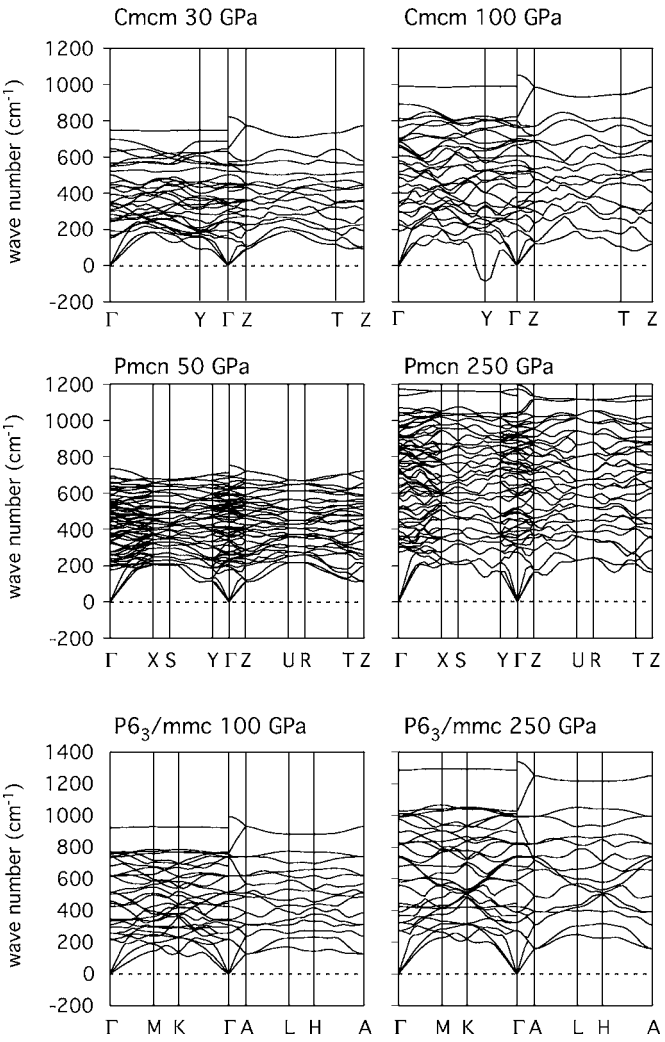

FIG. 3. Phonon dispersions of $NaMgF_3$. Pressures are static values.

The Mg coordination number in the $P6_3/mmc$ phase is 8, higher than 6 in the *Cmcm* and 7 in the *Pmcn* phases. The structural unit is no longer the MgF_6 octahedron but a MgF_8 parallelepiped, i.e., a distorted cube. Parallelepipeds share their edges to form layers in the *ab* plane. The layers contact adjacent ones at the parallelpipeds' apices along the [0001] direction. Na atoms are located at the interstitial sites between the MgF_8 parallelepipeds and the Na coordination number is 11. Na and Mg atoms stack in a *ABAC* sequence (A=Mg and B,C=Na), i.e., the sublattice formed by Na and Mg has the NiAs structure. The stacking sequence of F atoms is *ABCACB*. The Na and F sublattices have the $IrAl_3$ structure[13] in which the cation coordination number is 11. Enthalpy calculations show that the static transition pressure from *Pmcn* to $P6_3/mmc$ $NaMgF_3$ is 223 GPa [Fig. 7(b)]. From phonon dispersions (Fig. 3), we see that $P6_3/mmc$ $NaMgF_3$ is dynamically stable up to 300 GPa at least. Since there is no soft mode also in the *Pmcn* phase up to 250 GPa, the transition between *Pmcn* to $P6_3/mmc$ phases should be a regular enthalpically induced transition.

Figure 8 shows phase boundaries in the $NaMgF_3$ system. The boundaries between *Cmcm* and *Pmcn*, and *Pmcn* and

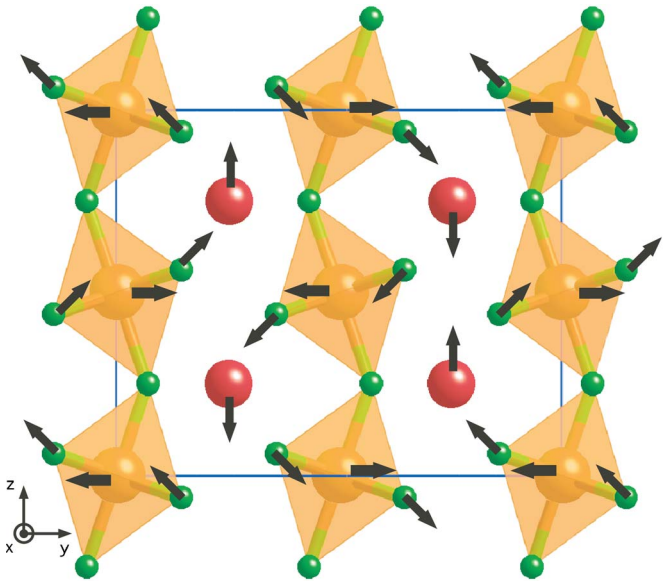

FIG. 4. (Color online) Atomic displacements resulting from the unstable phonon at the Y point of the Brillouin zone in *Cmcm* $NaMgF_3$ at 100 GPa (see Fig. 3).

$P6_3/mmc$ are metastable. They were computed using the quasi-harmonic approximation (QHA) to the free energy as a function of volume and temperature, $F(V,T)$:

$$F(V,T) = E_0(V) + \frac{1}{2}\sum_{i,\mathbf{q}} \hbar\omega_{i,\mathbf{q}}(V) + \sum_{i,\mathbf{q}} k_B T \times \log\left[1 - \exp\left(-\frac{\hbar\omega_{i,\mathbf{q}}(V)}{k_B T}\right)\right], \quad (1)$$

where $E_0(V)$ is the static total energy and $\omega_{i,\mathbf{q}}(V)$ are the phonon frequencies. The effect of the zero-point motion (ZPM) in the transition from *Cmcm* to *Pmcn* is very small. It changes the transition pressure from 43.5 GPa (static) to 43.3 GPa (0 K including ZPM). This is because the average phonon frequency [$\bar{\omega}=\int \omega f(\omega) d\omega$, where $f(\omega)$ is a vibrational density of states (VDOS) shown in Fig. 6] in the *Cmcm* and *Pmcn* phases is very similar, i.e., 433 and 431 cm^{-1}, respectively, at 50 GPa. Therefore the difference in the ZPM contribution to $F(V,T)$, according to the second term of Eq. (1), is very small. The Clapeyron slope of this metastable phase boundary is positive: 7.8 MPa/K at 500 K. The new bonds between layers increase especially the acoustic phonon frequencies; in Fig. 6(a), peaks at low phonon frequencies shift upward with the *Cmcm*-*Pmcn* transformation. Therefore, the relative stability of the *Pmcn* phase with respect to the *Cmcm* phase decreases with increasing temperature because of the third term of Eq. (1). In contrast, in the *Pmcn*-$P6_3/mmc$ phase boundary, ZPM decreases the transition pressure from 223 GPa (static) to 210 GPa (0 K including ZPM) and the Clapeyron slope is negative, −36 MPa/K at 500 K. At 250 GPa, $\bar{\omega}$ is 684 and 652 cm^{-1} for the *Pmcn* and $P6_3/mmc$ phases, respectively. The VDOS [Fig. 6(b)] shows that the $P6_3/mmc$ phase has a higher population of low-frequency phonons than the *Pmcn* phase.

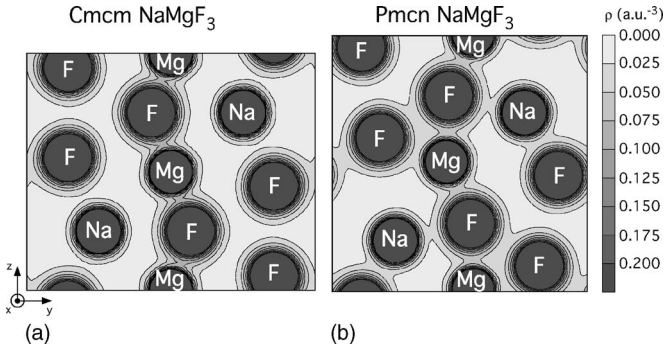

FIG. 5. Contour plots of valence charge densities on the (200) plane of *Cmcm* and *Pmcn* $NaMgF_3$ at 50 GPa.

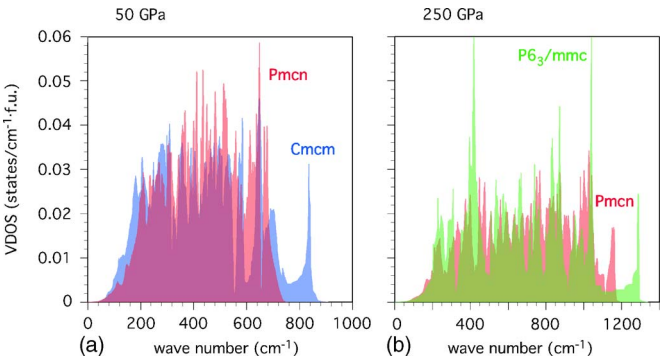

FIG. 6. (Color online) Comparison between vibrational densities of states (VDOSs) of (a) the *Cmcm* and *Pmcn* phases at 50 GPa and (b) the *Pmcn* and $P6_3/mmc$ phases at 250 GPa.

In general, pressure-induced transitions involve increase in cation coordination numbers and/or increase in polyhedral connectivity. Increase in cation coordination number occurs in all of these phase transitions. Increase in polyhedral connectivity occurs only in the observed *Pbnm*-*Cmcm* transition. With this in mind we investigated also other phases with increased degree of polyhedral connectivity. The natural candidates were $LiSbO_3$-type, $BaNiO_3$-type, and hexagonal $BaTiO_3$-type $NaMgF_3$.[13,14] The $LiSbO_3$-type structure consists of MgF_6 octahedra interconnected in an α-PbO_2-like

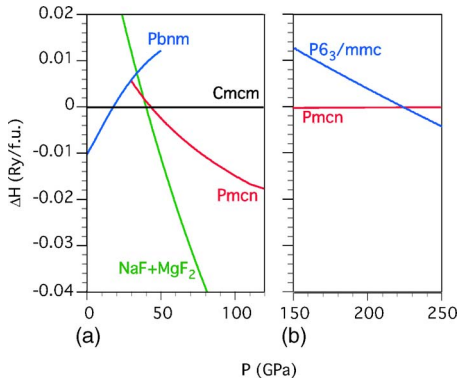

FIG. 7. (Color online) Relative static enthalpies of (a) *Pbnm* and *Pmcn* and the aggregation of CsCl-type NaF+cotunnite-type MgF_2 with respect to *Cmcm* $NaMgF_3$, and (b) $P6_3/mmc$ $NaMgF_3$ with respect to *Pmcn* $NaMgF_3$.

TABLE I. Lattice constants and atomic coordinates of *Pmcn* and $P6_3/mmc$ $NaMgF_3$. Pressures are static values. In *Pmcn* $NaMgF_3$, the inversion center is set at (1/4,1/4,0) for a simple comparison with the *Cmcm* phase.

	Cmcm $NaMgF_3$ at 30 GPa		
(*a*,*b*,*c*)	(2.772	8.682	6.877)Å
	x	*y*	*z*
Na (4*c*)	(0	0.2515	3/4)
Mg (4*a*)	(0	0	0)
F_1 (4*c*)	(0	0.9290	3/4)
F_2 (8*f*)	(0	0.3604	0.0601)
	Pmcn $NaMgF_3$ at 50 GPa		
(*a*,*b*,*c*)	(2.806	7.289	7.296)Å
	x	*y*	*z*
Na (4*c*)	(0	0.2529	0.8009)
Mg (4*c*)	(0	−0.0525	−0.0071)
F_1 (4*c*)	(0	0.9569	0.7344)
F_2 (4*c*)	(0	0.3859	0.0460)
F_3 (4*c*)	(0	0.3132	0.3983)
	$P6_3/mmc$ $NaMgF_3$ at 250 GPa		
(*a*,*c*)		(3.018	6.557)Å
	x	*y*	*z*
Na (2*d*)	(1/3	2/3	3/4)
Mg (2*a*)	(0	0	0)
F_1 (2*b*)	(0	0	1/4)
F_2 (4*f*)	(1/3	2/3	0.0803)

network, i.e., a multiple edge-sharing network. In $BaNiO_3$-type and hexagonal $BaTiO_3$-type structures, MgF_6 octahedra share faces. The enthalpies of these candidate phases are found to be higher than that of *Cmcm* $NaMgF_3$: relative enthalpies with respect to *Cmcm* $NaMgF_3$ at 50 GPa are 0.092, 0.173, and 0.128 Ry/f.u., respectively. Therefore it appears that an increase of MgF_6 octahedra's connectivity is not likely in $NaMgF_3$, except in the dissociation product.

III. CONCLUSIONS

We have identified two dynamically stable structures that are candidate ultrahigh pressure polymorphs of ABX_3-type compounds. They have *Pmcn* and $P6_3/mmc$ space groups. They are produced in *metastable* pressure-induced transformations in *Cmcm* $NaMgF_3$, a postperovskite phase. The first transition is related to a soft phonon mode in postperovskite, and the *Pmcn* space group is a subgroup of *Cmcm*. The second one is a regular enthalpically driven transition from *Pmcn* to $P6_3/mmc$. The latter is a supergroup of *Cmcm*. In

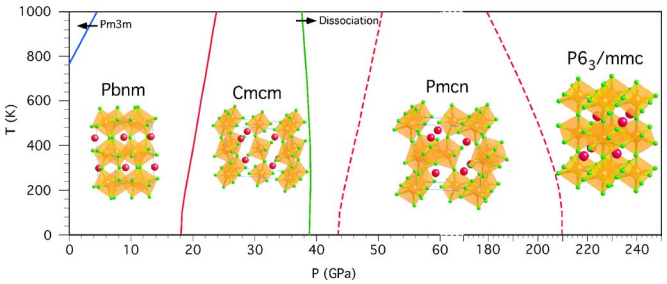

FIG. 8. (Color online) Calculated phase boundaries in $NaMgF_3$. The two dashed red lines denote the new metastable phase boundaries between *Cmcm* and *Pmcn* and between *Pmcn* and $P6_3/mmc$ phases, respectively. The phase boundaries of the PPV transition (solid red line) and the PPV dissociation (solid green line) are taken from Ref. 5. The solid blue line in the upper left corner denotes the experimental phase boundary between *Pbnm* and *Pm*3*m* phases (Ref. 15).

$NaMgF_3$ these phases are metastable with respect to the dissociation into CsCl-type NaF and cotunnite-type MgF_2.[5] However, other ABX_3-type compounds may favor these phases over the dissociation products. Even in $NaMgF_3$, the *Pmcn* phase might be observed under certain conditions. For instance, the enthalpy crossing between the *Cmcm* and *Pmcn* occurs just above the *Cmcm*-dissociation pressure. It is conceivable that the energy barrier for dissociation could be high to the point of allowing this transition to occur first, especially at low temperatures. Very recently Martin *et al.* reported diamond anvil cell experiments in *Cmcm* $NaMgF_3$ showing that new x-ray diffraction peaks occurred under pressure. However, these peaks could not be attributed only to a mixture of *Cmcm* and its dissociation products, NaF and MgF_2.[16] The superposition of peaks seems to be considerable and the analysis of the published pattern is challenging and inconclusive; but, the new x-ray diffraction pattern may contain peaks related to the *Pmcn* phase identified here.

In $MgSiO_3$ the enthalpy crossing between the *Cmcm* and *Pmcn* phases occurs beyond 1.6 TPa. This transition pressure is considerably higher than the dissociation pressure (1.1 TPa).[4] In nature these pressures are realized in the interior of the giants where temperatures are also very high 10^3-10^4 K. Therefore dissociation might not be inhibited in these environments and it is still the most likely pressure-induced transition in $MgSiO_3$ in the giants.

ACKNOWLEDGMENTS

Calculations have been done using the Quantum-ESPRESSO package.[17] Research was supported by NSF Grants EAR-0135533, EAR-0230319, and ITR-0426757 (VLab). Computations were performed at the Minnesota Supercomputing Institute.

[1] M. Murakami, K. Hirose, K. Kawamura, N. Sata, and Y. Ohishi, Science **304**, 855 (2004).
[2] T. Tsuchiya, J. Tsuchiya, K. Umemoto, and R. M. Wentzcovitch, Earth Planet. Sci. Lett. **224**, 241 (2004).
[3] A. R. Oganov and S. Ono, Nature (London) **430**, 445 (2004).
[4] K. Umemoto, R. M. Wentzcovitch, and P. B. Allen, Science **311**, 983 (2006).
[5] K. Umemoto, R. M. Wentzcovitch, D. Weidner, and J. Parise, Geophys. Res. Lett. **33**, L15304 (2006).
[6] J. P. Perdew and A. Zunger, Phys. Rev. B **23**, 5048 (1981).
[7] R. M. Wentzcovitch, Phys. Rev. B **44**, 2358 (1991).
[8] R. M. Wentzcovitch, J. L. Martins, and G. D. Price, Phys. Rev. Lett. **70**, 3947 (1993).
[9] P. Giannozzi, S. de Gironcoli, P. Pavone, and S. Baroni, Phys. Rev. B **43**, 7231 (1991).
[10] S. Baroni, S. de Gironcoli, A. Dal Corso, and P. Giannozzi, Rev. Mod. Phys. **73**, 515 (2001).
[11] D. Wallace, *Thermodynamics of Crystals* (Wiley, New York, 1972).
[12] D. Vanderbilt, Phys. Rev. B **41**, R7892 (1990).
[13] B. G. Hyde and S. Andersson, *Inorganic Crystal Structures* (Wiley, New York, 1989).
[14] R. W. G. Wyckoff, *Crystal Structures* (Interscience, New York, 1965), Vol. 2.
[15] Y. Zhao, D. J. Weidner, J. Ko, K. Leinenweber, X. Liu, B. Li, Y. Meng, R. E. G. Pacalo, M. T. Vaughan, Y. Wang, and A. Yeganeh-Haeri, J. Geophys. Res. **99** (B2), 2871 (1994).
[16] C. D. Martin, W. A. Crichton, H. Liu, V. Prakapenka, J. Chen, and J. B. Parise, Geophys. Res. Lett. **33**, L11305 (2006).
[17] S. Baroni, A. Dal Corso, S. de Gironcoli, P. Giannozzi, C. Cavazzoni, G. Ballabio, S. Scandolo, G. Chiarotti, P. Focher, A. Pasquarello, K. Laasonen, A. Trave, R. Car, N. Marzari, and A. Kokalj, http://www.pwscf.org/.